Virally Mediated Overexpression of Glial-Derived Neurotrophic Factor Elicits Age- and Dose-Dependent Neuronal Toxicity and Hearing Loss

Omar Akil,[1,*] Bas Blits,[2] Lawrence R. Lustig,[3] and Patricia A. Leake[1]

[1]Department of Otolaryngology—Head and Neck Surgery, University of California, San Francisco, San Francisco, California; [2]Department of Research and Development, UniQure Biopharma B.V., Amsterdam, The Netherlands; and [3]Department of Otolaryngology—Head and Neck Surgery, Columbia University Medical Center, New York, New York.

Contemporary cochlear implants (CI) are generally very effective for remediation of severe to profound sensorineural hearing loss, but outcomes are still highly variable. Auditory nerve survival is likely one of the major factors underlying this variability. Neurotrophin therapy therefore has been proposed for CI recipients, with the goal of improving outcomes by promoting improved survival of cochlear spiral ganglion neurons (SGN) and/or residual hair cells. Previous studies have shown that glial-derived neurotrophic factor (GDNF), brain-derived neurotrophic factor, and neurotrophin-3 can rescue SGNs following insult. The current study was designed to determine whether adeno-associated virus vector serotype 5 (AAV-5) encoding either green fluorescent protein or GDNF can transduce cells in the mouse cochlea to express useful levels of neurotrophin and to approximate the optimum therapeutic dose(s) for transducing hair cells and SGN. The findings demonstrate that AAV-5 is a potentially useful gene therapy vector for the cochlea, resulting in extremely high levels of transgene expression in the cochlear inner hair cells and SGN. However, overexpression of human GDNF in newborn mice caused severe neurological symptoms and hearing loss, likely due to Purkinje cell loss and cochlear nucleus pathology. Thus, extremely high levels of transgene protein expression should be avoided, particularly for proteins that have neurological function in neonatal subjects.

Keywords: glial-derived neurotrophic factor (GDNF), adeno-associated virus vector serotype 5 (AAV-5), hearing loss, spiral ganglion, auditory nerve, cochlear hair cells

INTRODUCTION

HEARING LOSS (HL) is the most common sensory disorder in the United States and usually manifests as an abnormality of the sensory epithelium and/or the auditory nerve. Etiologies underlying the degeneration of sensory cells and spiral ganglion neurons (SGNs) in the cochlea include genetic factors, mechanical stress, toxic insults, ischemia, and many others. Since the mammalian auditory epithelium is unable to replace lost sensory cells or SGN, sensorineural deafness due to loss of these cells is irreversible.[1–4] The loss of sensory cells leads to secondary degeneration of nerve fibers (NF) and eventually to the degeneration of SGN,[5–8] and recent studies have shown that primary neural degeneration can also occur with noise damage or aging.[9–11]

Patients with severe to profound hearing loss can often benefit from cochlear implantation (CI), but outcomes can be quite variable, with some CI recipients able to use the telephone and enjoy listening to music, whereas others receive very little benefit.[12,13] One important factor accounting for this variability in CI outcomes is the number or health of surviving SGN. Therefore, neurotrophin therapy has been proposed for CI recipients to promote improved neural and residual hair cell survival, thereby supporting optimum CI function. To date, there have been a number of reports of successful prevention or reduction of SGN degeneration in animal models using direct intracochlear delivery of neurotrophins (for review, see Staecker and Garnham[14] and Leake et al.[15]). Other studies

*Correspondence: Dr. Omar Akil, Department of Otolaryngology—Head and Neck Surgery, University of California, San Francisco, 533 Parnassus Avenue Room U490A, San Francisco, CA, 94143-0526. E-mail: omar.akil@ucsf.edu

have also demonstrated that neurotrophic agents can be combined successfully with electrical stimulation to promote improved neural survival and lower threshold in animal models, offering the potential for clinical therapies to improve CI outcomes.[16–18] Neurotrophins and their receptors have been shown to be expressed in both the developing and mature cochlea and to have an important role in the development of the auditory system.[19–28] In particular, brain-derived neurotrophic factor (BDNF) and neurotrophin-3 (NT-3) have been found in hair cells during development and in the mature organ of Corti.[19,29] Similarly, glial cell line–derived neurotrophic factor (GDNF), a potent survival factor for midbrain dopaminergic, spinal motor, cranial sensory, and sympathetic neurons,[30–32] has also been found in the inner ear. GDNF mRNA expression is seen in the SGN and the sensory epithelium of the developing inner ear in mammalian hair cells during development[33] and in the mature organ of Corti,[34] suggesting its potential role in the developing and mature cochlea. Additionally, mRNAs of GDNF receptors alpha and RET, the two receptors that are indispensable for GDNF function, have similarly been detected in the organ of Corti of mature rats.[35]

Many studies have shown that neurotrophins are capable of rescuing neurons following insult.[15,18,36,37] Infusion of GDNF into the cochlea via mini-osmotic pumps has been shown to improve survival of the SGN after deafness[38–41] and also to reduce cochlear hair cell damage caused by intensive noise in guinea pigs.[42,43] However, although osmotic mini-pumps are useful in animal models, they are less than ideal for clinical application with the goal of improving SGN populations for CI recipients[14,16,44] due to concerns about infection, rapid degradation, short-term function, and the tendency for high concentrations of neurotrophins to induce ectopic and disorganized sprouting of radial NF.[14–16,18,44] Consequently, there has been substantial recent interest in exploring alternative strategies for intracochlear delivery of NTs,[45,46] including cell-based therapies,[47–49] hydrogels,[50] and gene therapy using adenovirus-mediated expression of neurotrophic factors.[17,51–53] These methods are still in relatively early development, and concerns about potential side effects and risks have not yet been adequately addressed (for reviews, see Leake *et al.*,[18] Gillespie *et al.*,[54] and Staecker and Garnham[14]). Direct gene delivery to the cochlea offers the potential advantage of using a one-time injection to elicit sustained expression of neurotrophic factors by cells within the target tissue. Stable and long-term expression is particularly important in the cochlea,[55] given the slow time course of SGN degeneration in the human cochlea and the long duration of expected implant use (especially in pediatric CI recipients). Recombinant adeno-associated virus (AAV) was selected as the delivery vector for the current studies because it is non-replicating, can efficiently transfer transgenes to the inner ear, and causes no ototoxicity.[56–60] Other advantages of AAV are that it is not incorporated into the host genome, remains episomal, and results in stable, long-term expression of the transgene.[55] AAV has already been utilized in clinical applications for neurological and neuromuscular diseases without adverse effects, including injections into the eye to treat Leber's congenital amaurosis retinopathy.[60–63] Further, the cochlea is a favorable target organ for gene transfer because it is relatively isolated from surrounding tissues, resulting in limited viral spread and thus less exposure to the immune system. It may be particularly important to restrict GDNF gene transfer to the inner ear, since GDNF also functions in the kidneys and the central nervous system. Finally, inoculation of the cochlea with vectors is technically straightforward.

The aims of the current study were to determine whether AAV serotype 5 (AAV-5) encoding either the fluorescent marker green fluorescent protein (GFP) or the neurotrophin GDNF could transduce cells in the mouse cochlea; and to define the cell types transfected and to determine the optimum therapeutic dose(s) for eliciting robust GDNF expression in both hair cells and SGN. These studies will provide the basis for subsequent similar experiments in a deafened animal model to determine whether AAV-5-mediated GDNF expression can effectively promote survival of SGN, as shown with other delivery methods,[40,64–67] while avoiding the potentially deleterious disorganized radial nerve fiber sprouting seen with direct delivery of neurotrophins to the cochlea.[15,18,68] If successful, this work ultimately could lead to the development of a clinical therapy for preventing SGN/auditory nerve degeneration that would greatly benefit CI recipients and/or the development of a therapy to reconnect residual or regenerated hair cells to the SGN and auditory nerve.

MATERIALS AND METHODS
Animals

Wild-type (WT) FVB mice were purchased from Charles River Laboratories. Mice were housed and bred at the University of California, San Francisco, barrier facility. All procedures and animal handling were done according to approved national ethical guidelines and complied with all protocol requirements of the University of California

San Francisco Institutional Animal Care and Use Committee.

Hearing tests

Hearing tests were performed as previously described before[69] with treated (injected) and non-treated (control) mice littermates at different postnatal ages (P17 and P25 to P2 months). All auditory testing were performed in a soundproof chamber. Before acoustic testing, mice were anesthetized by intraperitoneal injection of a mixture of ketamine hydrochloride (Ketaset; 100 mg/mL) and xylazine hydrochloride (xyla-ject; 10 mg/mL), and supplements of one fifth the original dose were administered as required. Body temperature was monitored with a rectal probe throughout recording and maintained with a heating pad.

Auditory brainstem responses measurement. The evoked auditory brainstem responses (ABR) were differentially recorded from the scalp of the mice (treated and non-treated) using subdermal needle electrodes at the vertex, below the pinna of the left ear (reference) and below the contralateral ear (ground). The sound stimuli were 5 ms duration clicks delivered at 31 Hz. Measurements were made using the TDT BioSig III system (Tucker-Davis Technologies). For each stimulus, electro-encephalographic (EEG) activity was recorded for 20 ms at a sampling rate of 25 kHz and filtered (0.3–3 kHz), and waveforms from 512 stimuli were averaged for each response. ABR waveforms were recorded at a maximum stimulus level of ~ 90 dB sound pressure level (SPL) and then at 5 dB SPL decrements from the maximum intensity. The threshold was defined as the lowest stimulus level at which response peaks for waves I–V were clearly and reproducibly present upon visual inspection. These threshold judgments were confirmed by analysis of stored/averaged waveforms. Data were obtained from the treated mice and non-treated littermates at P17 for the mice injected at P1–3 and at varying ages, including P25, P40, and P60 for mice injected at P14.

To determine whether any changes in ABR latencies occurred, the ABR peaks and troughs were identified automatically by cursers programmed to identify each peak in the Tucker-Davis Technologies system software, and then verified by visual inspection of the recorded wave forms. The ABR waveforms latencies of waves I, II, and III were measured and analyzed in non-injected mice, in mice injected with AAV-5-GFP, and in mice injected with the 1:10 dilution of AAV-5-GDNF (mice injected with undiluted virus were totally deaf).

The comparisons among groups of animals were performed using one-way analysis of variance (ANOVA) with Bonferroni *post hoc* testing. Significance was defined at $p < 0.05$.

Compound action potential recording. Compound action potential (CAP) recording was performed, as previously described before.[70] A dorsal surgical approach[71] was used to expose the left cochlea of the treated mice ($n = 7$) and non-treated (control) littermates ($n = 5$) for recording. After making a small opening in the bulla and visualizing the round window niche, a fine recording electrode, fashioned from Teflon-coated insulated silver wire, was positioned in the niche and another was placed in the soft tissue of the neck as a ground electrode. The sound stimulus was generated with the Tucker-Davis System II hardware and software (Tucker-Davis Technologies). The CAP thresholds were measured in response to a click stimulus, and responses in the treated mice at P17 were compared to those obtained from non-treated littermates.

Viral construction

Recombinant AAV-5 vectors were manufactured by UniQure Biopharma B.V. with the chicken β-actin (CBA) promoter driving expression of GFP and human GDNF (hGDNF). The AAV-5 vectors were produced by dedicated procedures using the baculo-platform of UniQure. AAV-5-CBA-GFP was used at a titer of 1.4×10^{14} genome copies (gc)/mL and AAV-5-CBA-hGDNF at a titer of 1.8×10^{14} gc/mL.

Intracochlear injection

Intracochlear viral transduction was carried out, as described previously.[72] Normal WT FVB mice at P1–3 or at P14 were injected with AAV-5-GFP/hGDNF vectors directly into the scala tympani via the round window membrane. In anesthetized animals, a left post-auricular incision was made, and the otic bulla was exposed (and then opened, only in P14 animals). Next, a glass micropipette (10 μm outer tip diameter) containing 1–2 μL of the viral vector was inserted through the translucent bulla in P1–3 mice and through the round window membrane, and the viral preparation was then gently injected into the cochlea. After removing the pipette, the opening in the membrane was repaired with connective tissue and the incision sealed with tissue glue for P1–3-injected mice or with a 6-0 or smaller absorbable chromic suture for P14-injected mice.

RNA expression

Reverse transcriptase polymerase chain reaction. The total RNA harvested from both the

treated and non-treated mice cochleae extractions (Trizol™, Invitrogen) was reverse transcribed with superscript II RNase H⁻ (Invitrogen) for 50 min at 42°C using oligodT primers. Two microliters of RT reaction product was used for subsequent polymerase chain reaction (PCR; Taq DNA Polymerase, Invitrogen) of 35 cycles using the following parameters: 94°C for 30 s, 60°C for 45 s, 72°C for 1 min, followed by a final extension of 72°C for 10 min and storage at 4°C. Primers were designed to amplify a unique sequence of mouse *GDNF* (*mGDNF*) and *hGDNF*. To amplify *mGDNF* (BC119031), three sets of PCR primers pairs were tried: set 2/5—forward CCGGTAAGAGGCTTCTCGAA and reverse TTCCTGTGAATCGGCCGAGACAAT; set 4/3—forward AGGTCACCAGATAAACAAGC and reverse GTCTCGGAGTAGAAGGCTAACA; and set 6/1—forward CAGCGCTTCCTCGAAGAGAGA and reverse AACAAGTGACAAAGTAGGC. The primers were designed to amplify 393, 281, and 274 bp fragments, respectively. To amplify *hGDNF* (NM_001190468), three sets of PCR primers pairs were tried: set 2/5—forward CCGGTAAGAGGCCTCCCGAG and reverse CTCTTGCGATGCAGCTGAGACAAC; set 4/3—forward AGGTCACCAGATAAACAAAT and reverse ATC-CAGAAATAGAAGGCTGGTG; and set 6/1—forward CAGTGCTTCCTAGAAGAGAGC and reverse GGTGAGTGACAAAGTAGGG. These primers were designed to amplify 393, 281, and 274 bp fragments, respectively. Controls included cochlear RNA without reverse transcriptase. Analysis of each PCR sample was then performed on 2% agarose gels containing 0.5 μg/mL of ethidium bromide. Gels were visualized using a digital camera and image processing system (Kodak). Candidate bands were cut out, and the DNA was extracted (Qiaquick gel extraction kit, Qiagen) and sequenced (Elim Biopharmaceuticals, Inc.). The PCR product was then compared directly to the full mouse or *hGDNF* sequence for identification.

Quantitative PCR. For real-time quantitative PCR, cochleae from treated and non-treated mice were dissected, and RNA was extracted and processed for RT reaction, as described above. The expression level of *GDNF* was measured by the iQ5 real-time PCR system (Bio-Rad). Amplification was performed in a total volume of 25 μL containing 12.5 μL of SYBR Green I amplification master mix (Bio-Rad), 250 nM of primers (*mGDNF* [BC119031] forward AGGTCACCAGATAAACAAGC and reverse GTCTCGGAGTAGAAGGCTAACA primers were designed to amplify a 281 bp fragment; *hGDNF* [NM_001190468] forward AGGTCACCAGATAAACAAAT and reverse ATCCAGAAATAGAAGGCTGGTG primers were designed to amplify a

281 bp fragment; and mouse ribosomal protein L19 [BC083131] forward ATGTATCACAGCCTGTACCTG and reverse TTCTTGGTCTCTTCCTCCTTG primers were designed to amplify a 232 bp fragment), and 3 μL of 1:5 diluted cDNA as template. The amplifications were performed in triplicate wells using a protocol that consisted of initial denaturation at 95°C for 3 min followed by a 40-cycle denaturation at 95°C for 10 s and annealing at 61°C for 30 s. After amplification, a melting curve was generated for every PCR product to check the specificity of the PCR reaction (absence of primer dimers or other nonspecific amplification product). The $2^{-\Delta\Delta CT}$ method was used to calculate the relative fold difference between *hGDNF* and *mGDNF* expression determined from real-time quantitative PCR experiments normalized to the ribosomal RNA L19, an internal control, relative to the expression level of *mGDNF*.[73] Statistical differences were calculated using one-way ANOVA with Bonferroni *post hoc* test, with significance noted for $p < 0.05$.

Histology

Cochlea. Treated and non-treated mice littermates at P17 were anesthetized, and their cochleae were isolated, dissected, perfused through the round and oval windows with a solution of 2.5% paraformaldehyde and 1.5% glutaraldehyde in 0.1 M phosphate-buffered solution (PBS) at pH 7.4, and then placed in the same fixative overnight at 4°C. The cochlear specimens were rinsed with 0.1 M of PBS, post fixed in 1% osmium tetroxide for 2 h, rinsed again, and then immersed in 5% ethylenediaminetetraacetic acid (EDTA) for decalcification. The decalcified cochleae were then dehydrated in ethanol and propylene oxide, embedded in Araldite 502 resin (Electron Microscopy Sciences), and sectioned at 5 μm thickness parallel to the cochlear modiolus. Then sections were stained with toluidine blue and mounted with Permount (Thermo Fisher Scientific) on microscope slides and examined with a Leica microscope.

Cochlear nucleus. Treated and non-treated P17 mice were administered an overdose of a mixture of ketamine and xylazine, and transcardiac perfusion was performed with normal saline solution followed by a mixed aldehyde fixative (1.5% glutaraldehyde and 2.5% paraformaldehyde in 0.1 M of PBS, pH 7.4). The brain was removed from the skull, placed in the same fixative overnight, rinsed with PBS, and then transferred into a 40% sucrose solution in PBS for at least 72 h. The brains were rapidly frozen and sectioned serially on a cryostat in the coronal plane at a thickness of 20 μm. The individual sections were

mounted on 2% gelatin-coated glass slides and stained with 0.25% toluidine blue for histological assessment.

Immunofluorescence

Immunofluorescence of cochlear sections. Treated and non-treaded mice littermates at P17 were anesthetized, and their cochleae were isolated, dissected, perfused through the oval and round windows with 2% paraformaldehyde in 0.1 M of PBS at pH 7.4, and immersed in the same fixative for 2 h. After fixation, cochleae were rinsed with PBS and transferred to 5% EDTA in 0.1 M of PBS for decalcification. When the cochleae were completely decalcified (~2 days), they were incubated overnight in 30% sucrose for cryoprotection. The cochlear specimens then were embedded in O.C.T. Tissue Tek Compound (Miles Scientific) and cryosectioned parallel to the modiolus at 10–12 μm thickness for immunofluorescence. The sections were mounted on Superfrost™ microscope slides (Erie Scientific) and stored at –20°C until use. For immunofluorescent staining, cochlear sections from treated and non-treated mice were incubated overnight at 4°C with a rabbit anti-GFP antibody (Invitrogen A11122) diluted to 1:250 in PBS. The sections were then rinsed twice for 10 min with PBS, incubated for 2 h in goat anti-rabbit immunoglobulin G (IgG) conjugated to Cy2 (Jackson ImmunoResearch 111-165-003) diluted to 1:2,000 in PBS, rinsed again in PBS twice for 10 min, mounted on glass slides in a mounting solution containing DAPI, and observed under an Olympus microscope with confocal immunofluorescence.

Cochlear whole-mount immunofluorescence. Cochleae of treated and non-treated mice littermates were perfused with 4% paraformaldehyde in 0.1 M of PBS, pH 7.4, and placed in the same fixative for 2 h at 4°C. Cochleae were washed with PBS three times for 10 min and then decalcified with 5% EDTA in 0.1 M PBS for about 2 days. Following decalcification, the otic capsule was removed, followed by removal of the lateral wall, Reissner's membrane, and the tectorial membrane.

For GFP labeling, the remaining dissected specimen containing the organ of Corti (cochlear whole mount) was incubated in a humid chamber overnight at 4°C with a rabbit anti-GFP antibody (Invitrogen A11122) diluted to 1:250 in PBS. The cochlear whole mounts were rinsed twice for 10 min with PBS and then incubated for 2 h in goat anti-rabbit IgG conjugated to Cy2 diluted to 1:2,000 in PBS. Specimens were then rinsed with PBS, further microdissected into individual turns

(surface preparation), and incubated for 15 min at room temperature (RT) with the fluorescent DAPI to mark nuclei. The cochlear whole mounts were rinsed in PBS and mounted on glass slides in antifade FluorSave reagent (Calbiochem 34589). The organ of Corti and hair cells were examined with confocal immunofluorescence.

For neurofilament and synaptophysin double-labeling, the cochlear whole mounts were incubated in a humid chamber overnight at 4°C with the rabbit anti-neurofilament-200 antibody (1/500; NF-200; Chemicon), which labels afferent as well as some efferent auditory NF,[74] and mouse anti-synaptophysin antibody (1:200; Zymed), which predominantly labels efferent auditory fibers.[75] The specimens were then rinsed twice for 10 min and incubated for 2 h in goat anti-rabbit IgG conjugated to Cy2 (diluted to 1:2,000 in PBS) and goat anti-mouse IgG conjugated to Cy3 (diluted to 1:2,000 in PBS). The cochlear whole mounts were then rinsed in PBS twice for 10 min and processed the same way as for GFP labeling.

Cochlear nucleus immunofluorescence. Brains from the treated and non-treated mice at P17 were dissected and processed, as previously described, for histology. Brain sections were incubated overnight at 4°C with the rabbit anti-calbindin (a protein marker of the Purkinje cells), rinsed twice for 10 min with PBS, and then incubated for 2 h at RT with goat anti-rabbit IgG antibody conjugated to Cy3 (1:2,000 dilution in PBS; Jackson ImmunoResearch 111-165-003). Other brain sections were incubated overnight at 4°C with the rabbit anti-ionized calcium-binding adaptor 1 (Iba1) antibody (a glial cell marker), rinsed twice for 10 min with PBS, and then incubated for 2 h at RT with goat anti-rabbit IgG antibody conjugated to Cy2 (1:2,000 dilution in PBS; Jackson ImmunoResearch). The brain sections then were rinsed with PBS twice for 15 min and incubated for 15 min at RT with the fluorescent DAPI to mark nuclei. After another rinse in PBS, the sections were mounted on glass slides in antifade FluorSave reagent (Calbiochem 34589). The stained Purkinje cells were examined with an Olympus microscope with confocal immunofluorescence, and the glial cells were examined with a Zeiss microscope equipped with epifluorescence.

RESULTS

Assessment of the cell types transduced in the mouse cochlea and optimum therapeutic dose(s) for transfecting both hair cells and SGN after the delivery of AAV-5 encoding hGDNF would usually be determined by antibody-based assays (*e.g.*, immu-

nofluorescence). Unfortunately, the absence of a robust anti-hGDNF antibody makes this approach impossible. Instead, the GFP reporter gene was used to assess AAV-5 transfection within the cochlea.

Three different doses of AAV-5-GFP were used to estimate the optimum dose of AAV-5-hGDNF. The initial titer of the virus was 1.8×10^{14} gc/mL, and the doses evaluated were $2 \mu L$ of undiluted virus, $1 \mu L$ of undiluted virus, and $1 \mu L$ of a 1:10 dilution of the virus. WT FVB mice at P1–3 were injected with the AAV-5-GFP vector directly into the scala tympani through the round window membrane. Survival periods were approximately 2 weeks post injection. The study focused specifically on assessing the efficacy of transduction, types of cells transduced, and their distribution throughout the cochlea. Injections of both $2 \mu L$ and $1 \mu L$ of the undiluted AAV-5-GFP virus resulted in very strong expression in inner hair cells (IHC; about 80%) and much less expression in outer hair cells (OHC; <1%; Fig. 1A and B; IHC, white arrows; OHC, red arrows). Additionally, some pillar and other suppoting cells were seen to express GFP strongly at around 2 weeks post injection. SGN transfection also was assessed in sections cut in the mid-modiolar plane (Fig. 1C and D), and the data demonstrated strong expression in the majority of SGN (about 60%) in the injected (left) cochleae (Fig. 1C), whereas no SGN or hair cells expressed GFP in the control cochleae (Fig. 1D). No difference was noted between the injections of 2 versus $1 \mu L$. The lowest dosage (1:10 dilution) of the virus, however, resulted in significantly reduced transfection rates of all cell types (data not shown). Thus, $1 \mu L$ was selected as the dosage used for subsequent experiments with AAV-5-hGDNF.

Due to the lack of an effective antibody toward hGDNF to allow direct analysis of transfection and distribution by immunofluorescence, quantitative real-time PCR was used to study the relative levels of expression of the hGDNF induced compared to endogenous mGDNF mRNA expression. Initial studies verified the absence of cross-reactivity (Fig. 2A). Subsequent RT-PCR using cDNA from whole mouse cochlea following transfection with AAV-hGDNF showed expression of both hGDNF and endogenous mGDNF (Fig. 2B). The selected dose of $1 \mu L$ of undiluted virus resulted in ~ 1.43 million–fold amplification compared to native mGDNF mRNA expression (Fig. 2C). However, although the delivery of $1 \mu L$ of the undiluted AAV-5-GFP (1.4×10^{14} gc/mL) resulted in higher hair cell and SGN transfection rates without any adverse effects, by 12 days post injection of AAV-5-
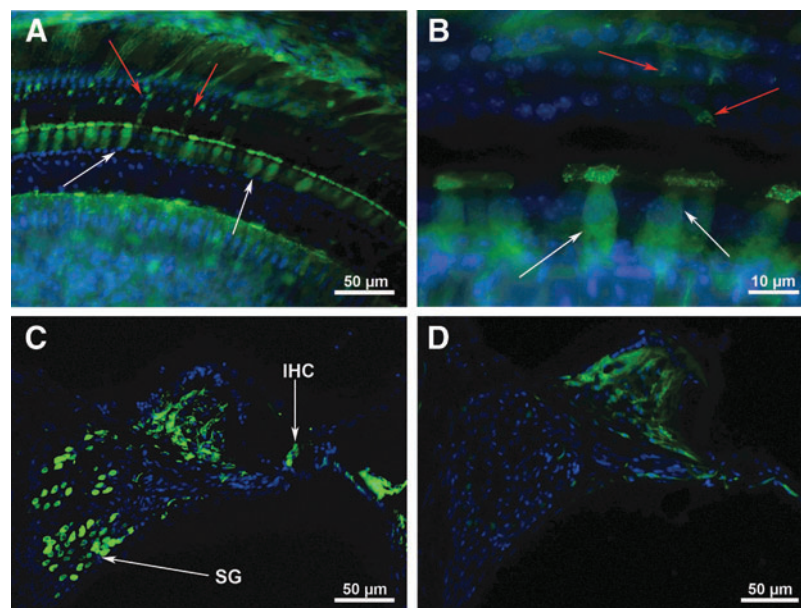

Figure 1. Adeno-associated virus serotype 5 (AAV-5)-green fluorescent protein (GFP) transfection of the cochlea. Three concentrations of virus were studied: undiluted, 1:10 dilution, and 1:20 dilution. As expected, $1 \mu L$ of the undiluted virus resulted in the highest level of inner hair cells (IHC), outer hair cells (OHC), and spiral ganglion neurons (SGN) cell transfection. **(A)** Two weeks following transfection, numerous transfected IHCs (*white arrows*) and a few OHCs (*red arrows*) in addition to some pillar and supporting cells strongly express GFP. **(B)** Higher magnification of the transfected IHC (*white arrows*) in the same mouse cochlea as shown in **(A)**. **(C)** Mid-modiolar section from the injected left cochlea demonstrates transfection of the IHC (*arrow*). Further, most of the SGN in the field also strongly express GFP. **(D)** Mid-modiolar section of the contralateral, untreated right cochlea, showing no GFP expression in IHC, OHC, or SGN.
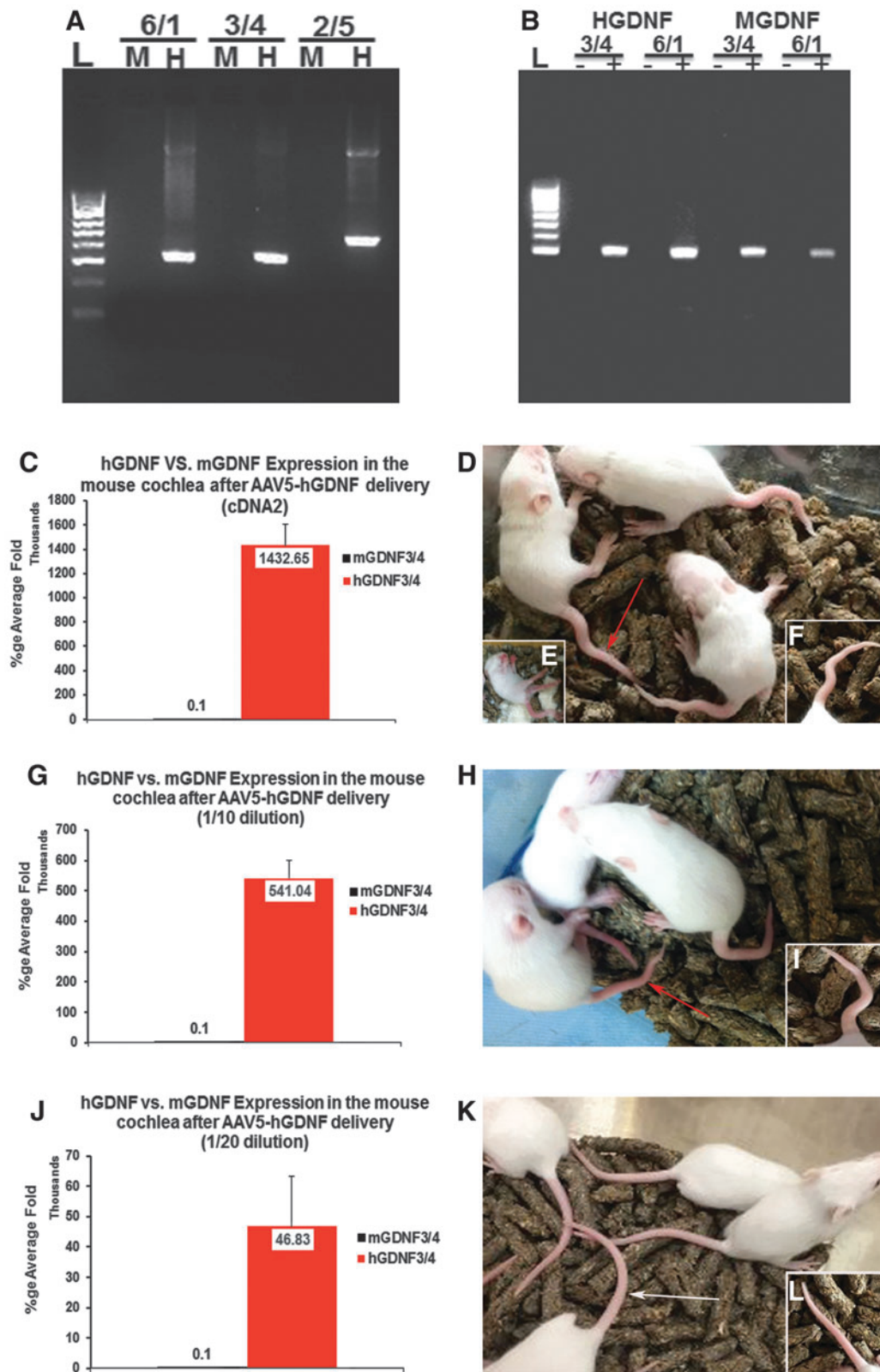
Figure 2. Human glial-derived neurotrophic factor (hGDNF) mRNA expression following AAV-5-hGDNF delivery to the cochlea. Polymerase chain reaction (PCR) using an expression vector containing hGDNF as a template demonstrated that the mouse (m)GDNF (M) primers (6/1, 3/4, and 2/5) do not amplify the hGDNF (H) gene **(A)**. Reverse transcription PCR using cDNA from the mouse cochlea after injection of AAV-hGDNF **(B)** showed expression of both hGDNF when using two different sets of human primers (H: 3/4 and 6/1) and endogenous mGDNF when using two different sets of mouse primers (M: 3/4 and 6/1). Reactions without reverse transcriptase (−) were used as negative controls. Quantitative real-time PCR (qPCR) data were obtained 2 weeks after intracochlear injections in P1–3 mice of AAV-5-hGDNF at different dilutions (undiluted, 1/10, 1/20). **(C–F)** Data from 1 μL of undiluted AAV-5-hGDNF injections: Mice displayed neurological symptoms (tremors, poor coordination, ataxia, malformed tails) at P12, which became lethal starting at ∼P17 **(D–F)**. At around P17, qPCR data showed that hGDNF was expressed at 1.43 million–fold compared to mGDNF **(C)**. **(G–I)** One microliter of 1:10 diluted AAV5-hGDNF: Mice showed no neurological symptoms or mortality, but did have minor tail deformities **(H** and **I)**. The qPCR data revealed high levels of expression of hGDNF relative to mGDNF, around 541,040-fold amplification **(G)**. **(J–L)** Data after 1 μL of 1:20 diluted AAV5-hGDNF. Mice look similar to non-injected controls **(K** and **L)**. The qPCR data still show high levels of expression of hGDNF relative to mGDNF, at around 46,830-fold amplification **(J)**.
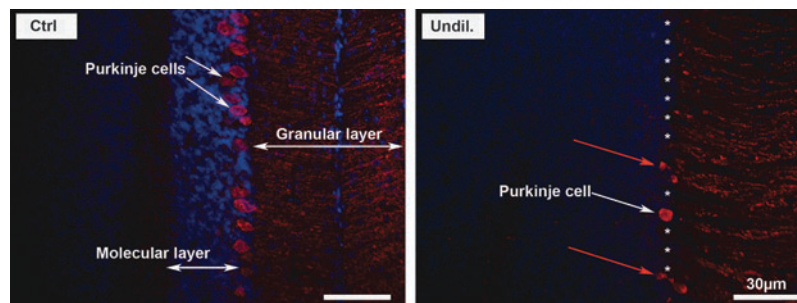
Figure 3. hGDNF overexpression causes damage to the cerebellar Purkinje cells. Immunofluorescence staining of brain sections using anti-calbindin (a protein marker of the Purkinje cells) revealed strong labeling of the cerebellar Purkinje cell somata in the control, and loss of the Purkinje cells in the undiluted AAV5-hGDNF transfection group. This loss of Purkinje cells may explain some of the neurologic symptoms observed (tremors, poor coordination, and ataxia). *White asterisks* indicate the approximate locations of missing Purkinje cells, and *red arrows* show abnormal Purkinje cells in the treated mice.

hGDNF, the pups were exhibiting significant neurological symptoms, including shaking/tremors, signs of ataxia, and malformations of their tails (Fig. 2C and D), which became lethal starting at around P17. In an attempt to mitigate these complications, more dilute preparations of virus were tested subsequently, including 1:10 and 1:/20 dilutions. With the 1:10 dilution, hGDNF showed approximately 541,000-fold amplification over native mGDNF, and at this lower concentration, mice showed no neurological symptoms except minor tail deformities and no mortality (Fig. 2G–I). With injections of the 1:20 dilution of the virus, hGDNF expression was approximately 48,600-fold compared to mGNDF, and at this dilution, mice were indistinguishable from (non-injected) controls (Fig. 2J–L).

To investigate potential mechanisms underlying the severe neurological impairment (tremors, poor coordination, ataxia, and malformed tails) observed in mice injected with undiluted AAV-5-hGDNF, the cerebellum was examined in P17-treated and control mice. Specifically, brain specimens were frozen-sectioned and stained with an anti-calbindin antibody (a protein marker of the Purkinje cells), and the cerebellum was studied under fluorescent microscopy. It was found that many Purkinje cells were missing in the injected compared to the non-injected mice (Fig. 3), which may at least partly explain the cause of the neurological symptoms seen in the
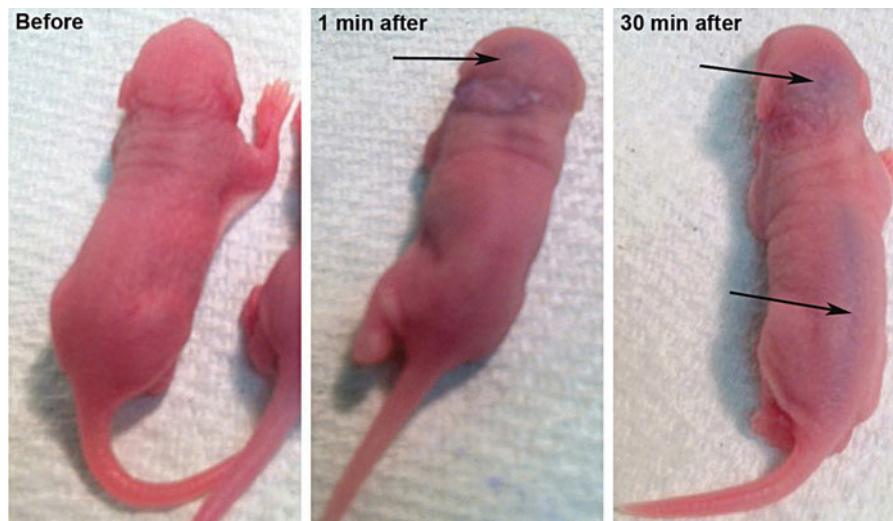

Figure 4. Diffusion of a visible dye into the spinal cord after round window injection in newborn mice. Time lapse photographs after intracochlear injection of a visible biological dye (*blue*) demonstrated diffuse spread into the spinal cord over a relatively short time period. The likely route of egress from the cochlea is through a patent cochlear aqueduct. This finding may explain the tail deformities and central nervous system changes seen with high levels of hGDNF expression.

newborn injected mice. This loss of Purkinje cells may be attributed to the hGDNF overexpression.

To gain a better understanding of how the AAV-5-hGDNF virus reached the cerebellum, newborn mice were injected with a biological dye into the left ear through the round window membrane. Time elapse photographs of mice following intracochlear injection (Fig. 4) demonstrated diffuse spread into the brain and the spinal cord within minutes, likely through a patent cochlear aqueduct at this young age. This finding may explain not only the loss of the Purkinje cells, but also the tail deformities seen with extremely high levels of hGDNF expression.

Brain sections from the control and the treated mice immunostained with Iba1 antibody, a glial cell marker, demonstrated that the glial cells of the control mice were faintly stained not only in the cochlear nucleus (CN) but throughout the whole brain section, indicative of the resting form of the glial cells (Fig. 7C low magnification and Fig. 7D high magnification). The brains of the treated mice demonstrated proliferation of glial cells not only in the CN but also throughout the entire brain section (Fig. 7C low magnification and Fig. 7D high mag-

nification). The glial cells in the brains of treated mice exhibited a hypertrophic phenotype with larger cell bodies compared to the brains of control mice, which is suggestive of an activated state of the glial cells, presumably to regulate inflammation and minimize brain injury caused by the GDNF overexpression.

Given the severity of the neurological symptoms, hearing and weight loss were also evaluated in additional mice that were transfected with these same dilutions of virus, studied at P17, and compared to control (non-transfected) mice. Hearing loss was assessed by determining ABR thresholds, and these data were compared to the body weights at the P17 endpoint (Fig. 5). Mice that received the undiluted AAV-hGDNF virus were profoundly deaf, and body weights were only about 50% of normal mice. The 1:10 dilution group showed a significant elevation in ABR threshold and weighed about 70% of normal. The 1:20 dilution group was relatively similar to the control mice, with no significant change in ABR threshold and only a slight loss of body weight (Fig. 5A). In contrast, mice receiving AAV-5-GFP showed no significant changes
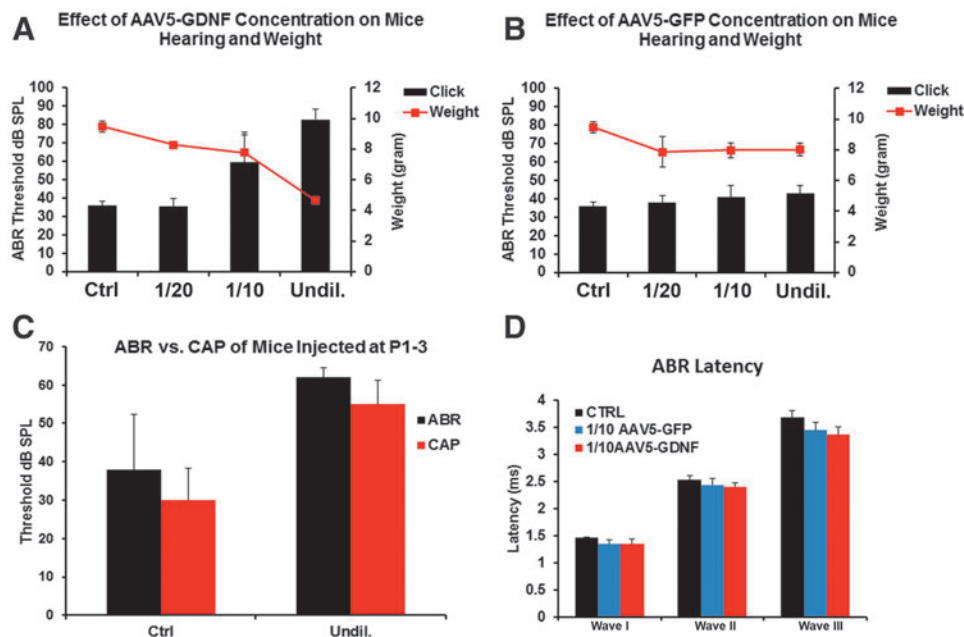

Figure 5. hGDNF overexpression causes hearing and weight loss. **(A)** Auditory brainstem response (ABR) thresholds (*black bars*) and body weights (*red line*) were measured in P17 mice 2 weeks after AAV5-hGDNF injections and compared to controls (CTRL). A majority of the mice injected with the undiluted (Undil.) virus showed profound hearing loss, and body weights were only around 50% of normal. The 1:10 dilution group showed a significant elevation in ABR thresholds and around 30% lower body weights relative to normal mice. The 1:20 dilution group was similar to the control mice, with no significant hearing loss and only a slight reduction in body weight. **(B)** ABR threshold and body weight did not show significant differences between the control group and the groups injected with AAV5-GFP, demonstrating the virus itself does not cause the pathological changes seen. **(C)** Compound action potential (CAP) thresholds also showed significant differences between the control group and the group injected with undiluted AAV5-hGDNF. ABR waveform latencies of waves I, II, and III between non-injected mice (CTRL), mice injected with 1:10 AAV5-GFP, and mice injected with 1:10 AAV5-hGDNF **(D)** did not show any significant changes. These results indicate that the speed of transmission, the hearing signal, was not affected in the AAV5-GDNF-injected mice from the cochlea to the cochlear nucleus.
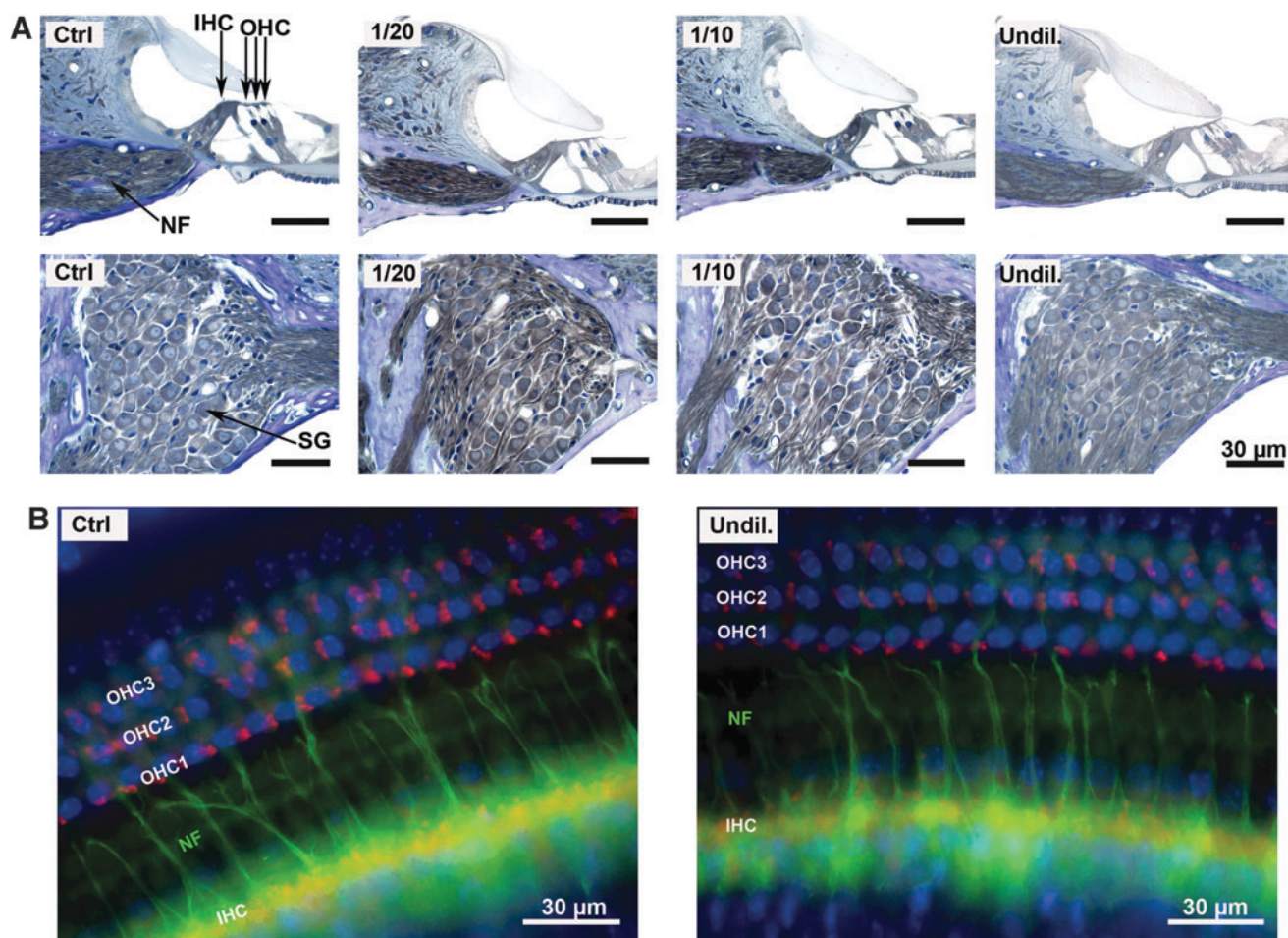
Figure 6. Cochlear sensorineural structures in mice after injection of AAV5-hGDNF appear normal, despite hearing loss. **(A)** Histology of mouse cochlear sections stained with toluidine blue 2 weeks after injection of AAV5-hGDNF revealed no gross abnormalities in the organ of Corti, IHCs, OHCs, nerve fibers (NF), or SGNs, suggesting that the overexpression of hGDNF does not affect the cochlear structures. **(B)** Cochlear whole mount immunofluorescence revealed no visible loss of OHC or IHC (DAPI stain = blue) in the undiluted AAV5-hGDNF injected group. Synaptophysin (*red*) and neurofilament (*green*) label shows similar staining patterns between the control (CTRL) and the injected ears, which indicates that the overexpression of the hGDNF does not grossly affect the sensorineural structures of the cochlea. Thus, the hearing loss may be due to central effects of hGDNF.

in any parameter measured, regardless of which virus dilution was given, demonstrating that it was the hGDNF, and not the virus, that was responsible for the changes seen with hGNDF transfection (Fig. 5B).

To identify more precisely the location of the hearing deficits recorded in sound-evoked potentials in the mice injected with undiluted and 1:10 diluted AAV-5-hGDNF, auditory nerve compound action potentials (CAP) were recorded at the round window at P17 and compared to the CAPs of the non-injected mice (Fig. 5C). Under these conditions, the injected mice CAP thresholds were significantly elevated, similar to what was seen with the ABR, indicating that cochlear dysfunction underlies at least some of the hearing loss observed.

To determine whether there were changes in the ABR waveforms, the ABR waveform latencies of

waves I, II, and III of the treated mice were measured and analyzed, but only for mice injected with 1:10 dilution (because the mice injected with undiluted virus were totally deaf). These results did not show any significant changes in ABR waveform latencies of waves I, II, and III between the control mice, mice injected with 1:10 AAV-5-GFP, and mice injected with 1:10 AAV-5-hGDNF (Fig. 5D).

To explore the potential causes of hearing loss in the AAV-5-hGDNF-injected mice further, the cochleae of P17 mice were examined with light microscopy. Standard histological analysis of mid-modiolar sections of the organ of Corti and spiral ganglion region from the middle cochlear turn demonstrated no gross abnormalities, with apparently normal numbers and morphology of IHC, OHC, cochlear NF, and SGN (Fig. 6A). In addition, cochlear whole mount preparations were examined

with double-label immunofluorescence using an anti-synaptophysin antibody (red), which labels efferent auditory fibers, and anti-neurofilament antibody (green), which labels afferent and efferent auditory fibers to look for any abnormalities in the cochlear hair cell synapses and NF. These studies documented identical staining patterns in control ears and ears injected with undiluted virus (Fig. 6B), and also demonstrated no visible loss of IHCs or OHCs (DAPI stain, blue).

Given the normal organ of Corti morphology, next, the study sought to determine whether the cochlear nucleus was affected by hGDNF over-expression by examining toluidine blue–stained frozen brain sections containing the ventral cochlear nuclear complex (VCN) of injected and non-injected (control) mice (Fig. 7). Although low magnification imaging did not reveal any major anatomical differences, higher magnification images suggested abnormal cells that appeared larger and misshapen in the injected versus control mice. These results suggest that at least some of the hearing loss seen in the hGNDF-injected animals may be due to central nervous system (CNS) changes.

Lastly, the study sought to determine whether the neurological symptoms seen in the hGDNF-injected mice (higher titer delivery), including shaking/tremors, signs of ataxia, kinks or tortuous malformations of their tails, weight loss, and hearing loss, were specific to mice injected as newborns or whether similar complications would be seen when the virus was injected into adult mice when the patency of the cochlear aqueduct would be expected to be reduced or eliminated. To address this question, intracochlear injections of undiluted AAV-5-hGDNF were made in mice at P14. When injections of the undiluted virus were made in these older animals, the hGDNF did not cause any of the concerning neurological symptoms that were observed following injections in newborn mice. However, a small but significant threshold shift (5–10 dB) and significant weight loss were observed at about P25 and remained unchanged thereafter through P60 (Fig. 8).

DISCUSSION

There has been great interest in recent years in potential therapies to induce cellular regeneration of the inner ear to prevent or reverse the degenerative effects of sensorineural hearing loss. Initial successful attempts at delivering therapeutic agents in animals have included the use of osmotic mini-pumps or direct injection of the recombinant protein into the scala tympani. However, thera-

peutic proteins administered via a bolus injection or pumps are challenged by infection, rapid degradation, and short-term function. These problems may be overcome by the use of gene transfer methods. Direct gene delivery into the cochlea offers the potential for stable and long-term gene expression after a single injection of a viral vector. To date, the vector that has shown the greatest promise for long-term transgene expression is AAV, which is non-pathologic and nontoxic, with proven safety and efficacy in several human gene therapy studies. However, one drawback of AAV may be the limitations in cell types that can be transfected. An ideal gene therapy vector must be suited to the target cells (*e.g.*, IHC and/or OHC, SGN, or the stria vascularis). Most AAV serotype vectors tested thus far have shown robust IHC transfection, with variable degrees of OHC and SGN transfection.[76,77] Thus, the search continues for ideal vectors that transfect a number of different cell types within the inner ear. Toward that end, this study sought to determine whether these AAV-5 vectors that were produced by dedicated procedures using the baculo-platform of UniQure could effectively transduce cells within the cochlea. There was a particular interest in determining whether the SGN could be efficiently transfected, as GDNF transfection of these cells may have a potential clinical role in promoting improved neural survival.

Many studies have shown that GDNF is a potent neuronal growth and survival factor, which has been considered for clinical use in the treatment of Parkinson's disease[78–81] and is capable of rescuing neurons following insult.[36,37] Infusion of GDNF into the inner ear has been shown to reduce cochlear hair cell lesions caused by intensive noise exposure in guinea pigs,[42,43] making it a good candidate to study in mice in order to define the optimum therapeutic dose(s) for transfecting both hair cells and SGN. These studies should provide the basis for subsequent similar experiments in a deafened animal model to determine whether AAV-mediated GDNF expression can effectively promote survival of SGN, as shown with other delivery methods,[40,64–67] while avoiding infection, rapid degradation, short-term function, and potentially deleterious disorganized radial nerve fiber sprouting seen with direct inner-ear delivery of neurotrophins.[15,18,68]

Following delivery of the AAV-5 vector coding for GFP (AAV-5-GFP) into the inner ear via the round window membrane of newborn mice, strong GFP expression was observed in IHCs (about 80%) and SG neurons (about 60%) throughout the cochlea, with modest expression in OHCs and supporting cells (Fig. 1). The data corroborate previous studies
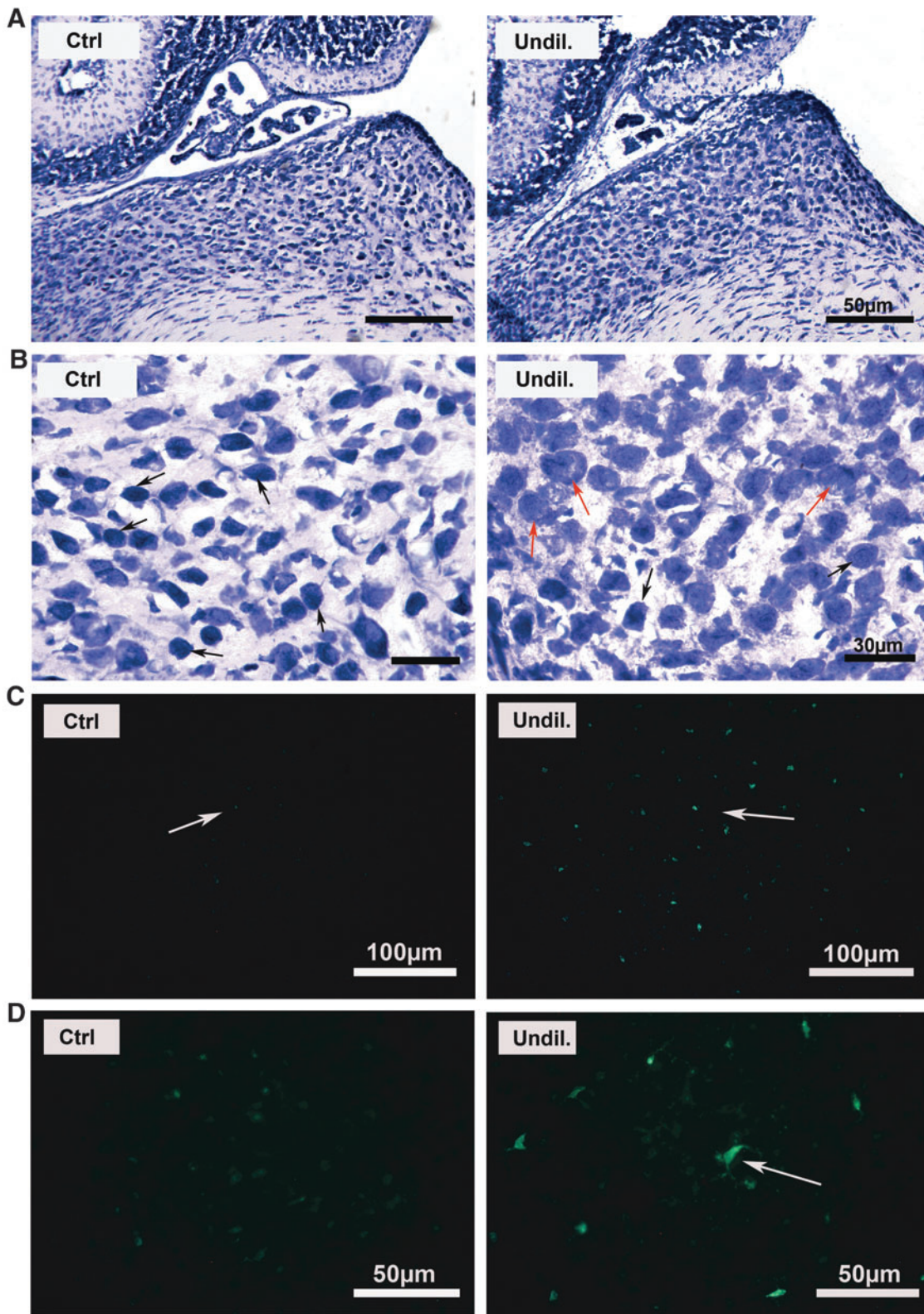
Figure 7. Cochlear nucleus cellular morphology is altered in mice after injection of AAV5-hGDNF. **(A)** An overview of brain sections (toluidine blue staining) illustrating the ventral cochlear nucleus (VCN) of treated and non-treated (control) mice. At this low magnification, no obvious changes in the treated mice are apparent. **(B)** At higher magnification, cells in the VCN of mice treated with AAV5-hGDNF appear swollen and misshapen compared to the control mice. Immunofluorescence images showing the glial cells stained with ionized calcium-binding adaptor 1 antibody (Iba1; a glial cells marker) in the brains of control and treated **(C** and **D)** mice. Iba1 (*green*) stained glial cells in the brains of treated mice exhibit a hypertrophic phenotype with larger cell bodies when compared to the brains of control mice. *Arrows* indicate proliferated glial cells in the treated brain.
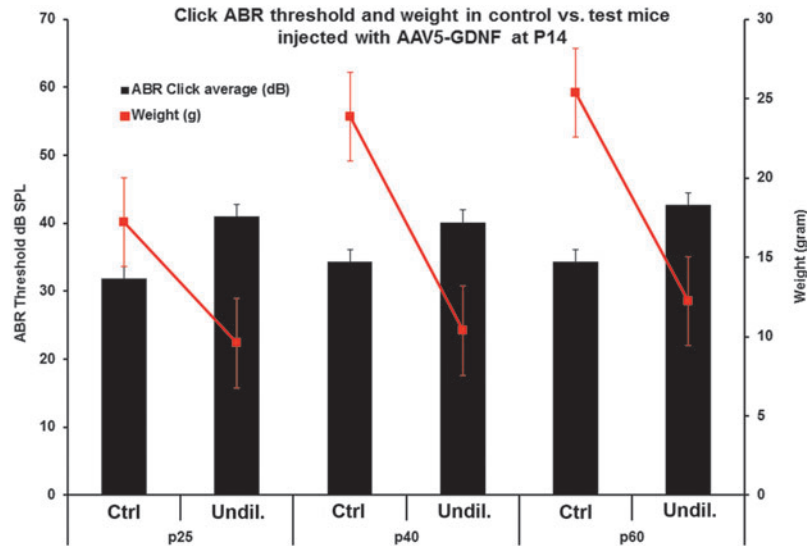
Figure 8. Adverse neurologic changes are avoided when older animals are transfected. ABR thresholds and body weights were measured at P25, P40, and P60 after AAV5-hGDNF injections at P14 (undiluted) and in non-injected (control) mice. Most of the mice injected with the undiluted virus showed a slight hearing loss (around 10 dB) and significant reduced body weight (10–15 g) compared to the control mice. No neuronal symptoms were observed in these mice.

on the distribution of transduced cells in the inner ear following inoculation of AAV-5-GFP vectors.[76,82] Testing three different doses of AAV-5-GFP, $1\,\mu L$ of AAV-5-GFP (1.4×10^{14}) was noted to be optimal based on the highest IHC and SGN transfection rates. It was thus assumed that this would similarly be the optimal dosage for AAV-5-hGDNF vector. It seemed likely that the AAV-5-hGDNF vector would transduce a population of cells similar to those transfected by the reporter gene and with a similar transfection rate and similar viral capsid used. These cells are presumed to synthesize excess hGDNF and secrete it, making it available to other cells in the inner ear, such as other nearby SGN that are not directly transduced. Due to the lack of a good anti-GDNF antibody to allow direct analysis of transfection and distribution by immunofluorescence, quantitative real-time PCR was used to determine the relative levels of expression of the hGDNF induced compared to endogenous mGDNF mRNA expression. The selected dose of $1\,\mu L$ of AAV-5-hGDNF of undiluted virus resulted in an extremely robust ~ 1.43 million–fold amplification compared to native mGDNF mRNA expression (Fig. 2C) without any initial adverse effects. In contrast, by 12 days post injection of $1\,\mu L$ of the AAV-5-hGDNF, the pups were exhibiting significant neurological symptoms, including shaking/tremors, signs of ataxia, and tortuous malformations of their tails (Fig. 2C and D), which later became lethal. Using serial dilutions of AAV-5-hGDNF, it was possible to reduce

or eliminate the neurological symptoms caused by the hGDNF overexpression while still generating high levels of hGDNF expression and transfection rates (around 48,000-fold expression in the 1:20 dilution studies).

This study addressed several important questions. Is AAV-5 a good candidate vector to be used for cochlear gene therapy? These studies show that robust IHC and SGN transfection rates with high levels of transgene expression make it a good choice if the target is these cell types. The answer to the second question addressed in this study—whether GDNF is a potential candidate for hearing preservation therapy—is not as clear. These studies show that robust overexpression of hGDNF in a newborn mouse causes a number of severe neurological malformations, leading to death by P17. These affects can be mitigated by diluting the viral load delivered or by delivering the viral vector at a later age, presumably when the cochlear aqueduct is smaller or closed. In humans, this may be an irrelevant issue, as the cochlear aqueduct is not thought to be patent after birth.[83] Yet, even with a 1:20 dilution of the virus, a level that eliminated neurologic deficits in the treated mice, there was still a 48,000-fold amplification of hGDNF over native mGDNF. This suggests that even further dilutions might achieve a sufficient level of GDNF expression for clinical efficacy, though the effect of such greater dilution on transfection rates is as yet unknown. All of these issues would clearly need to be addressed before considering such a therapy in humans.

An interesting question that arose in this study is how hGDNF overexpression led to the severe neurologic impairment seen (tremors, poor coordination, ataxia, and malformed tails). Toward this end, frozen sections of the cerebellum of P17-treated and control mice were examined using an anti-calbindin antibody (a protein marker of the Purkinje cells). It was found that many Purkinje cells were missing in the brains of injected compared to non-injected mice (Fig. 3). This loss of Purkinje cells may be attributed to hGDNF overexpression and may at least partly explain the neurological symptoms seen in the newborn-injected mice. The nature of these effects was largely consistent with previous studies conducted with GDNF in monkeys,[78] in which it was demonstrated that cerebellar injury occurred only in animals treated with the highest evaluated dose, and the lesion appeared mainly as Purkinje cell loss. This cerebellar lesion has not been reported in association with hGDNF treatment in rodent or other nonhuman primate studies described in the published literature.[84–88] This dose-related finding strongly suggests that the lesion was a hGDNF-mediated phenomenon. The underlying mechanism for this effect is not clear. However, it is known that the cerebellar Purkinje cells are vulnerable to multiple insults. Consequently, their loss is common to many pathologic conditions,[89] including global ischemia.[90,91] It was also reported that when ibogaine or harmaline are administered systemically (intraperitoneally) to rats, they produce ataxia and tremor that is associated with neuronal degeneration limited almost exclusively to the cerebellum.[92–95] Furthermore, within the cerebellum, the damage is specific to Purkinje cells and their dendrites.[93,94] Purkinje cells are the only efferent projections of the cerebellar cortex through their inhibitory (GABAergic) interaction with the deep cerebellar nuclei that project to upper motorneurons in the cortex (through the thalamus) and brain stem.[89,96,97] Because the cerebellum modulates movement via this efferent pathway, the loss of Purkinje cells leads to functional deficits. Cerebellar damage is known to be associated with abnormalities in gait and posture, limb movement deficits (including ataxia and intention tremor), dysarthria, and oculomotor disturbances across species.[89,97–99] Thus, it appears likely that the motor deficits and tail deformities seen in the treated animals in this study are due to damage to Purkunje cells.

To gain a better understanding of how the AAV-5-hGDNF virus reached the cerebellum, a biological dye was injected into the left ear of newborn mice to see if the virus crossed into the CNS via direct spread. This experiment demonstrated diffuse spread into the brain and the spinal cord (Fig. 4), likely through a patent cochlear aqueduct at this young age, suggesting that the AAV-5-hGDNF or secreted hGDNF reached the cerebrospinal fluid circulation in sufficient concentration to result in the distribution of hGDNF throughout the brain and the spinal cord.[100,101] Previous data in a study of VGLUT3[102] also demonstrated that the AAV virus can reach the CN and express the transgene RNA and protein in the CN cells. Based on these data, it is assumed that there is a direct effect of hGDNF on the CNS.

This finding may explain not only the loss of the Purkinje cells but also the tail deformities seen with extremely high levels of hGDNF expression. Interestingly, the tail deformities closely resemble the *meander tail* mutant mouse (*mea*), described as an autosomal recessive mutation whose phenotype is characterized by mild ataxia and a skeletal abnormality resulting in a kinked tail[103] that are attributed to the profound disorganization of the cerebellar cytoarchitecture.

In addition, the glial cells in the brains of treated mice exhibited a hypertrophic phenotype with larger cell bodies compared to the brains of control mice. This finding is suggestive of an activated state of the glial cells, presumably to regulate inflammation and minimize brain injury[104–108] caused by the GDNF overexpression. These results are in agreement with a previous study in the CN demonstrating microglial activation in response to trauma.[109]

Given the severity of the neurological symptoms, hearing and weight loss were also assessed in these mice. Mice that received the undiluted AAV-5-hGDNF virus were profoundly deaf, and body weights were only about 50% of normal mice. In contrast, the 1:10 dilution group showed a significant elevation in ABR threshold and weighed about 70% of normal, and the 1:20 dilution group was relatively similar to the control mice, with no significant change in ABR threshold and only a slight loss of body weight (Fig. 5A). In contrast, mice receiving AAV-5-GFP showed no significant changes in any parameter measured, regardless of which virus dilution was given, suggesting that it was the hGDNF, and not the virus, that was responsible for the changes seen (Fig. 5B). Whether the body weight reduction is due to reduced food consumption[78] or another effect of hGDNF is unclear at present.

To determine whether there were changes in the ABR waveforms, the latencies of waves I, II, and III were measured and analyzed in the mice injected with the 1:10 dilution of AAV-5-GDNF (the mice injected with undiluted virus were totally deaf).

These results (Fig. 5D) did not show any significant changes in latencies for any of the waveforms between the control mice, the mice injected with 1:10 AAV-5-GFP, and the mice injected with 1:10 AAV-5-hGDNF. These results suggest that the speed of transmission of the auditory input was not affected in the AAV-5-GDNF-injected mice, at least up to the point at which the fibers enter the cochlear nucleus.

To explore the nature of the hearing loss recorded further, auditory nerve CAPs were recorded and compared to the CAPs of control mice (Fig. 5C). The CAP thresholds in the injected mice were significantly elevated, similar to the elevation in thresholds seen with the ABR. This suggests that cochlear dysfunction underlies at least some of the hearing loss observed, although the standard histological analysis of mid-modiolar sections of the organ of Corti and SG region failed to reveal any gross abnormalities, and showed normal numbers and morphology of IHC, OHC, cochlear NF, and SGN (Fig. 6A). In addition, anti-synaptophysin and anti-neurofilament stains of cochlear whole mounts demonstrated no abnormalities of cochlear synapses or efferent auditory fibers of the ears injected with undiluted AAV-5-hGDNF virus (Fig. 6B), nor any visible loss of IHCs or OHCs (DAPI stain, blue). Given the normal organ of Corti morphology, next, the study sought to determine whether the cochlear nucleus was obviously affected by hGDNF overexpression by examining toluidine blue–stained frozen brain sections containing VCN of injected and control mice (Fig. 7). Examination of these histological sections of VCN suggested the presence of abnormal cells that appeared larger and misshapen in the injected mice. These results suggest that at least some of the hearing loss seen in the hGNDF-injected animals may also be due to pathological alteration in the CNS. Other studies have shown that cerebellar Purkinje cells and Schwann cell hyperplasia can occur in the presence of nerve growth factor.[78,110–112] Thus, it is possible that a similar mechanism is responsible for the VCN changes seen here.

Finally, intracochlear injections of undiluted AAV-5-hGDNF that were performed in mice at P14 did not cause any of the concerning neurological symptoms that were observed following injections in newborn mice. However, a small but significant threshold shift (5–10 dB) and significant weight loss were observed at about P25 and P60 (Fig. 8) in these animals. Previous studies conducted on adult rodents or nonhuman primates did not report any of these symptoms associated with hGDNF treatment[84–88] except weight loss. These results suggest

that the neurological symptoms observed were specific to mice injected as newborns. The profound effect seen at this early age may be due to increased delivery of hGDNF via a patent cochlear aqueduct, which was not seen at later ages in this or other studies, or may be an effect of GDNF exposure to the CNS at such a young age. A similar phenomenon of CNS sensitivity to early drug exposure was observed in a rat model[113] when anticonvulsant drug therapy was given during critical periods of brain development, and which severely affected neurodevelopmental outcomes and triggered neuronal apoptosis. Further, these results are consistent with other reports of anesthesia-induced white matter apoptosis during brain development. For example, phenobarbital and phenytoin, two of the most commonly utilized drugs for neonatal seizures,[114] trigger profound neuronal apoptosis in developing rodent models.[115–119]

In conclusion, AAV-5 represents a potentially useful gene therapy vector for the cochlea, eliciting extremely high levels of transgene expression in the cochlear IHCs and SGN. However, the overexpression of hGDNF in newborn mice can cause severe neurological symptoms and hearing loss due to Purkinje cell loss and cochlear nucleus pathology. Thus, extremely high levels of transgene protein expression should be avoided, particularly for proteins that may have neurological function when injected in neonatal subjects. These data also suggest that intracochlear injection of AAV encoding for neurotrophic factors may provide a viable delivery method in clinical trials for hearing restoration and protection once optimal dosing parameters can be established. Lastly, if AAV-mediated GDNF expression can be shown in further studies to promote survival of SGN effectively, then the intracochlear delivery of AAV-5-GDNF as reported in this study may have potential clinical application for improving CI performance.

AUTHOR DISCLOSURE

The authors declare no competing financial interests.

REFERENCES

1. Hudspeth AJ. How hearing happens. Neuron 1997;19:947–950.

2. Roberson DW, Rubel EW. Cell division in the gerbil cochlea after acoustic trauma. Am J Otol 1994;15:28–34.

3. Hawkins JE Jr. Comparative otopathology: aging, noise, and ototoxic drugs. Adv Otorhinolaryngol 1973;20:125–141.

4. Spoendlin H. Retrograde degeneration of the cochlear nerve. Acta Otolaryngol 1975;79:266–275.

5. Bichler E, Spoendlin H, Rauchegger H. Degeneration of cochlear neurons after amikacin intoxication in the rat. Arch Otorhinolaryngol 1983; 237:201–208.

6. Jyung RW, Miller JM, Cannon SC. Evaluation of eighth nerve integrity by the electrically evoked middle latency response. Otolaryngol Head Neck Surg 1989;101:670–682.

7. Koitchev K, Guilhaume A, Cazals Y, et al. Spiral ganglion changes after massive aminoglycoside treatment in the guinea pig. Counts and ultrastructure. Acta Otolaryngol 1982;94:431–438.

8. Webster DB, Webster M. Multipolar spiral ganglion neurons following organ of Corti loss. Brain Res 1982;244:356–359.

9. Liberman LD, Suzuki J, Liberman MC. Dynamics of cochlear synaptopathy after acoustic overexposure. J Assoc Res Otolaryngol 2015;16:205–219.

10. Kujawa SG, Liberman MC. Synaptopathy in the noise-exposed and aging cochlea: primary neural degeneration in acquired sensorineural hearing loss. Hear Res 2015;330:191–199.

11. Fernandez KA, Jeffers PW, Lall K, et al. Aging after noise exposure: acceleration of cochlear synaptopathy in "recovered" ears. J Neurosci 2015;35:7509–7520.

12. Holden LK, Finley CC, Firszt JB, et al. Factors affecting open-set word recognition in adults with cochlear implants. Ear Hear 2013;34:342–360.

13. Drennan WR, Rubinstein JT. Music perception in cochlear implant users and its relationship with psychophysical capabilities. J Rehabil Res Dev 2008;45:779–789.

14. Staecker H, Garnham C. Neurotrophin therapy and cochlear implantation: translating animal models to human therapy. Exp Neurol 2010;226:1–5.

15. Leake PA, Hradek GT, Hetherington AM, et al. Brain-derived neurotrophic factor promotes cochlear spiral ganglion cell survival and function in deafened, developing cats. J Comp Neurol 2011;519:1526–1545.

16. Shepherd RK, Coco A, Epp SB. Neurotrophins and electrical stimulation for protection and repair of spiral ganglion neurons following sensorineural hearing loss. Hear Res 2008;242: 100–109.

17. Chikar JA, Colesa DJ, Swiderski DL, et al. Overexpression of BDNF by adenovirus with concurrent electrical stimulation improves cochlear implant thresholds and survival of auditory neurons. Hear Res 2008;245:24–34.

18. Leake PA, Stakhovskaya O, Hetherington A, et al. Effects of brain-derived neurotrophic factor (BDNF) and electrical stimulation on survival and function of cochlear spiral ganglion neurons in deafened, developing cats. J Assoc Res Otolaryngol 2013;14:187–211.

19. Pirvola U, Ylikoski J, Palgi J, et al. Brain-derived neurotrophic factor and neurotrophin 3 mRNAs in the peripheral target fields of developing inner ear ganglia. Proc Natl Acad Sci U S A 1992;89: 9915–9919.

20. Pirvola U, Arumae U, Moshngakow M, et al. Coordinated expression and function of neurotrophins and their receptors in the rat inner ear during target innervation. Hear Res 1994;75:131–144.

21. Farinas I, Jones KR, Backus C, et al. Severe sensory and sympathetic deficits in mice lacking neurotrophin-3. Nature 1994;369:658–661.

22. Jones KR, Farinas I, Backus C, et al. Targeted disruption of the BDNF gene perturbs brain and sensory neuron development but not motor neuron development. Cell 1994;76:989–999.

23. Ernfors P, Lee KF, Jaenisch R. Mice lacking brain-derived neurotrophic factor develop with sensory deficits. Nature 1994;368:147–150.

24. Ernfors P, Van De Water T, Loring J, et al. Complementary roles of BDNF and NT-3 in vestibular and auditory development. Neuron 1995;14:1153–1164.

25. Despres G, Romand R. Neurotrophins and the development of cochlear innervation. Life Sci 1995;54:1291–1297.

26. Liu X, Ernfors P, Wu H, et al. Sensory but not motor neuron deficits in mice lacking NT4 and BDNF. Nature 1995;375:238–241.

27. Fritzsch B, Barald KF, Lomax MI. Early embryology of the vertebrate ear. In: Rubel EW, Popper AN, Fay RR, eds. Development of the Auditory System: Springer Handbook of Auditory Research. New York: Springer-Verlag, 1997:80–145.

28. Fritzsch B, Pirvola U, Ylikoski J. Making and breaking the innervation of the ear: neurotrophic support during ear development and its clinical implications. Cell Tissue Res 1999;296:369–382.

29. Ylikoski J, Pirvola U, Moshnyakov M, et al. Expression patterns of neurotrophin and their receptor mRNAs in the rat inner ear. Hear Res 1993;65:69–78.

30. Lin LF, Doherty DH, Lile JD, et al. GDNF a glial cell line-derived neurotrophic factor from midbrain dopaminergic neurons. Science 1993;260: 1130–1132.

31. Buj-Bello A, Buchman VL, Horton A, et al. GDNF is an age-specific survival factor for sensory and autonomic neurons. Neuron 1995;15:821–828.

32. Trupp M, Rydén M, Jörnvall H, et al. Peripheral expression and biological activities of GDNF, a new neurotrophic factor for avian and mammalian peripheral neurons. J Cell Biol 1995;130:137–148.

33. Nosrat CA, Tomac A, Lindqvist E, et al. Cellular expression of GDNF mRNA suggests multiple functions inside and outside the nervous system. Cell Tissue Res 1996;286:191–207.

34. Ylikoski J, Pirvola U, Virkkala J, et al. Guinea pig auditory neurons are protected by glial cell line-derived growth factor from degeneration after noise trauma. Hear Res 1998;124:17–26.

35. Stöver T, Gong TL, Cho Y, et al. Expression of the GDNF family members and their receptors in the mature rat cochlea. Mol Brain Res 2000;76:23–35.

36. Hakuba N, Watabe K, Hyodo J, et al. Adenovirus-mediated overexpression of a gene prevents hearing loss and progressive inner hair cell loss after transient cochlear ischemia in gerbils. Gene Ther 2003;10:426–433.

37. Havenith S, Versnel H, Aqterberg MJ, et al. Spiral ganglion cell survival after round window membrane application of brain-derived neurotrophic factor using gelfoam as carrier. Hear Res 2011;272:168–177.

38. Kanzaki S, Stöver T, Kawamoto K, et al. Glial cell line-derived neurotrophic factor and chronic electrical stimulation prevent VIII cranial nerve degeneration following denervation. J Comp Neurol 2002;454:350–360.

39. Yagi M, Kanzaki S, Kawamoto K, et al. Spiral ganglion neurons are protected from degeneration by GDNF gene therapy. J Assoc Res Otolaryngol 2000;1:315–325.

40. Maruyama J, Miller JM, Ulfendahl M. Glial cell line-derived neurotrophic factor and antioxidants preserve the electrical responsiveness of the spiral ganglion neurons after experimentally induced deafness. Neurobiol Dis 2008;29:14–21.

41. Glueckert R, Bitsche M, Miller JM, et al. Deafferentation-associated changes in afferent and efferent processes in the guinea pig cochlea and afferent regeneration with chronic intrascalar brain-derived neurotrophic factor and acidic fibroblast growth factor. J Comp Neurol 2008;507:1602–1621.

42. Yamasoba T, Schacht J, Shoji F, et al. Attenuation of cochlear damage from noise trauma by an iron chelator, a free radical scavenger and glial cell line-derived neurotrophic factor *in vivo*. Brain Res 1998;815:317–325.

43. Keithley EM, Ma CL, Ryan AF, et al. GDNF protects the cochlea against noise damage. Neuroreport 1998;9:2183–2187.

44. Gillespie LN, Shepherd RK. Clinical application of neurotrophic factors: the potential for primary auditory neuron protection. Eur J Neurosci 2005; 22:2123–2133.

45. Hendricks JL, Chikar JA, Crumling MA, et al. Localized cell and drug delivery for auditory prostheses. Hear Res 2008;242:117–131.

46. Richardson RT, Wise AK, Andrew JK, et al. Novel drug delivery systems for inner ear protection and regeneration after hearing loss. Expert Opin Drug Deliv 2008;5:1059–1076.

47. Warnecke A, Wissel K, Hoffmann A, et al. The biological effects of cell-delivered brain-derived neurotrophic factor on cultured spiral ganglion cells. Neuroreport 2007;29:18:1683–1686.

48. Pettingill LN, Minter RL, Shepherd RK. Schwann cells genetically modified to express neurotrophins promote spiral ganglion neuron survival *in vitro*. Neuroscience 2008;27:152:821–828.

49. Wise AK, Fallon JB, Neil AJ, et al. Combining cell-based therapies and neural prostheses to promote neural survival. Neurotherapeutics 2011;8:774–787.

50. Endo T, Nakagawa T, Kita T, et al. Novel strategy for treatment of inner ears using a biodegradable gel. Laryngoscope 2005;115:2016–2020.

51. Nakaizumi T, Kawamoto K, Minoda R, et al. Adenovirus-mediated expression of brain-derived neurotrophic factor protects spiral ganglion neurons from ototoxic damage. Audiol Neurootol 2004;9:135–143.

52. Rejali D, Lee VA, Abrashkin KA, et al. Cochlear implants and *ex vivo* BDNF gene therapy protect spiral ganglion neurons. Hear Res2007;228:180–187.

53. Wise AK, Hume CR, Flynn BO, et al. Effects of localized neurotrophin gene expression on spiral ganglion neuron resprouting in the deafened cochlea. Mol Ther 2010;18:1111–1122.

54. Gillespie LN, Clark GM, Bartlett PF, et al. BDNF-induced survival of auditory neurons *in vivo*: cessation of treatment leads to accelerated loss of survival effects. J Neurosci Res 2003;71:785–790.

55. Xia L, Yin S, Wang J. Inner ear gene transfection in neonatal mice using adeno- associated viral vector: a comparison of two approaches. PLoS One 2012;7:e43218.

56. Husseman J, Raphael Y. Gene therapy in the inner ear using adenovirus vectors. Adv Otorhinolaryngol 2009;66:37–51.

57. Ballana E, Wang J, Venail F, et al. Efficient and specific transduction of cochlear supporting cells by adeno-associated virus serotype 5. Neurosci Lett 2008;442:134–139.

58. Konishi M, Kawamoto K, Izumikawa M, et al. Gene transfer into guinea pig cochlea using adeno-associated virus vectors. J Gene Med 2008;10:610–618.

59. Praetorius M, Brough DE, Hsu C, et al. Adenoviral vectors for improved gene delivery to the inner ear. Hear Res 2009;248:31–38.

60. Lustig LR, Akil O. Cochlear gene therapy. Curr Opin Neurol 2012;25:57–60.

61. Bennett J, Ashtari M, Wellman J, et al. AAV2 gene therapy readministration in three adults with congenital blindness. Sci Transl Med 2012; 4:120ra15.

62. Simonelli F, Maguire AM, Testa F, et al. Gene therapy for Leber's congenital amaurosis is safe and effective through 1.5 years after vector administration. Mol Ther 2010;18:643–650.

63. Grieger JC, Samulski RJ. Adeno-associated virus vectorology, manufacturing, and clinical applications. Meth Enzymol 2012;507:229–254.

64. Wefstaedt P, Scheper V, Lenarz T, et al. Brain-derived neurotrophic factor/glial cell line-derived neurotrophic factor survival effects on auditory neurons are not limited by dexamethasone. Neuroreport 2005;16:2011–2014.

65. Wei D, Jin Z, Järlebark L, et al. Survival, synaptogenesis, and regeneration of adult mouse spiral ganglion neurons *in vitro*. Dev Neurobiol 2007;67:108–122.

66. Scheper V, Paasche G, Miller JM, et al. Effects of delayed treatment with combined GDNF and continuous electrical stimulation on spiral ganglion cell survival in deafened guinea pigs. J Neurosci Res 2009;87:1389–1399.

67. Fransson A, Maruyama J, Miller JM, et al. Post-treatment effects of local GDNF administration to the inner ears of deafened guinea pigs. J Neurotrauma 2010;27:1745–1751.

68. Stöver T, Scheper V, Diensthuber M, et al. *In vitro* neurite outgrowth induced by BDNF and GDNF in combination with dexamethasone on cultured spiral ganglion cells. Laryngorhinootologie 2007;86:352–357.

69. Akil O, Chang J, Hiel H, et al. Progressive deafness and altered cochlear innervation in knockout mice lacking prosaposin. J Neurosci 2006;26:13076–13088.

70. Seal RP, Akil O, Yi E, et al. Sensorineural deafness and seizures in mice lacking vesicular glutamate transporter 3. Neuron 2008;57:263–275.

71. Akil O, Rouse SL, Chan DK, et al. Surgical method for virally mediated gene delivery to the mouse inner ear through the round window membrane. J Vis Exp 2015;16.

72. Akil O, Seal RP, Burke K, et al. Restoration of hearing in the VGLUT3 knockout mouse using virally mediatedgene therapy. Neuron 2012;75: 283–293.

73. Livak KJ, Schmittgen TD. Analysis of relative gene expression data using real-time quantitative PCR and the 2(-Delta Delta C (T)) method. Methods 2001;25:402–408.

74. Berglund AM, Ryugo DK. Neurofilament antibodies and spiral ganglion neurons of the mammalian cochlea. J Comp Neurol 1991;306:393–408.

75. Schimmang T, Tan J, Muller M, et al. Lack of Bdnf and TrkB signalling in the postnatal cochlea leads to a spatial reshaping of innervation along the tonotopic axis and hearing loss. Development 2003;130:4741–4750.

76. Kilpatrick LA, Li Q, Yang J, et al. Adeno-associated virus-mediated gene delivery into the scala media of the normal and deafened adult mouse ear. Gene Therapy 2011;18:569–578.

77. Askew C, Rochat C, Pan B, et al. Tmc gene therapy restores auditory function in deaf mice. Sci Transl Med 2015;7:295ra108.

78. Hovland D, et al. Six-month continuous intraputamenal infusion toxicity study of recombinant methionyl human glial cell line–derived neurotrophic factor (r-metHuGDNF) in rhesus monkeys. Toxicol Pathol 2007;35:1013–1029.

79. Richardson RM, Kells AP, Rosenbluth KH, et al. Interventional MRI-guided putaminal delivery of AAV2-GDNF for a planned clinical trial in Parkinson's disease. Mol Ther 2011;19:1048–1057.

80. Kells AP, Forsayeth J, Bankiewicz KS. Glial-derived neurotrophic factor gene transfer for Parkinson's disease: anterograde distribution of AAV2 vectors in the primate brain. Neurobiol Dis 2012;48 228–235.

81. San Sebastian W, Richardson RM, et al. Safety and tolerability of magnetic resonance imaging-guided convection-enhanced delivery of AAV2-hAADC with a novel delivery platform in nonhuman primate striatum. Hum Gene Ther 2012;23:210–217.

82. Liu Y, Okada T, Sheykholeslami K, et al. Specific and efficient transduction of cochlear inner hair cells with recombinant adeno-associated virus type 3 vector. Mol Ther 2005;12:725–733.

83. Gopen Q, Rosowski JJ, Merchant SN. Anatomy of the normal human cochlear aqueduct with functional implications. Hear Res 1997; 107:9–22.

84. Gash DM, Zhang Z, Cass W, et al. Morphological and functional effects of intranigrally administered GDNF in normal rhesus monkeys. J Comp Neurol 1995;363:345–358.

85. Gash DM, Zhang Z, Ovadia A, et al. Functional recovery in Parkinsonian monkeys treated with GDNF. Nature 1996;380:252–255.

86. Bjorklund A, Rosenblad C, Winkler C, et al. Studies on neuroprotective and regenerative effects of GDNF in a partial lesion model of Parkinson's disease. Neurobiol Dis 1997;4:186–200.

87. Rosenblad C, Kirik D, Bjorklund A. Sequential administration of GDNF into the substantia nigra and striatum promotes dopamine neuron survival and axonal sprouting but not striatal reinnervation or functional recovery in the partial 6-OHDA lesion model. Exp Neurol 2000;161:503–516.

88. Grondin R, Zhang Z, Yi A, et al. Chronic, controlled GDNF infusion promotes structural and functional recovery in advanced Parkinsonian monkeys. Brain 2002;125:2191–2201.

89. Fonnum F, Lock EA. Cerebellum as a target for toxic substances. Toxicol Lett 2000; 112–113:9–16.

90. Brierley JB, Excell BJ. The effects of profound systemic hypotension upon the brain of M. rhesus: physiological and pathological observations. Brain 1966;89:269–298.

91. Brierley JB, Brown AW, Excell BJ, et al. Brain damage in the rhesus monkey resulting from profound arterial hypotension. I. Its nature, distribution and general physiological correlates. Brain Res 1969;13:68–100.

92. Singbartl G, Zetler G, Schlosser L. Structure–activity relationships of intracerebrally injected tremorigenic indole alkaloids. Neuropharmacology 1973;12:239–244.

93. O'Hearn E, Long DB, Molliver ME. Ibogaine induces glial activation in parasagittal zones of the cerebellum. Neuroreport 1993;4:299–302.

94. O'Hearn E, Molliver ME. Degeneration of Purkinje cells in parasagittal zones of the cerebellar vermis after treatment with ibogaine or harmaline. Neuroscience 1993;55:303–310.

95. O'Hearn E, Molliver ME. Neurotoxins and neuronal death: an animal model of excitotoxicity. In: Koliatsos VE, Ratan RR, eds. Cell Death and Diseases of the Nervous System. Totowa, NJ: Humana Press, Inc., 1999;221–245.

96. Welsh JP, Yuen G, Placantonakis DG, et al. Why do Purkinje cells die so easily after global brain ischemia? Aldolase C, EAAT4, and the cerebellar contribution to posthypoxic myoclonus. Adv Neurol 2002;89:331–359.

97. Sarna JR, Hawkes R. Patterned Purkinje cell death in the cerebellum. Prog Neurobiol 2003; 70:473–507.

98. Gemba H, Sasaki K, Yoneda Y, et al. Tremor in the monkey with a cerebellar lesion. Exp Neurol 1980;69:173–182.

99. Trouillas P, Takayanagi T, Hallett M, et al. International Cooperative Ataxia Rating Scale for pharmacological assessment of the cerebellar syndrome. The Ataxia Neuropharmacology Committee of the World Federation of Neurology. J Neurol Sci 1997;145:205–211.

100. Raphael R, Ciuman MD. Communication routes between intracranial spaces and inner ear: function, pathophysiologic importance and relations with inner ear diseases. Am J Otolaryngol Head Neck Med Surg 2009;30:193–202.

101. Salt AN, Gill RM, Hartsock JJ. Perilymph kinetics of FITC-Dextran reveals homeostasis dominated by the cochlear aqueduct and cerebrospinal fluid. J Assoc Res Otolaryngol 2015;16:357–371.

102. Akil O, Kiringoda R, Seal R, et al. Unilateral cochlear delivery of virally mediated gene therapy demonstrates bilateral expression and function in VGLUT3 knockout mice. Poster 39th ARO Meeting, 2016; PS#346 p62.

103. Hollander WF, Waggie KS. Meander tail: a recessive mutant located in chromosome 4 of the mouse. J Hered 1977;68:403–406.

104. Bruce-Keller AJ. Microglial-neuronal interactions in synaptic damage and recovery. J Neurosci Res 1999;58:191–201.

105. Mrak RE, Griffin WS. Glia and their cytokines in progression of neurodegeneration. Neurobiol Aging 2005;26:349–354.

106. Cullheim S, Thams S. The microglial networks of the brain and their role in neuronal network plasticity after lesion. Brain Res Rev 2007;55:89–96.

107. Hanisch UK, Kettenmann H. Microglia: active sensor and versatile effector cells in the normal and pathologic brain. Nat Neurosci 2007;10: 1387–1394.

108. Skaper SD. The brain as a target for inflammatory processes and neuroprotective strategies. Ann N Y Acad Sci 2007;1122:23–34.

109. Baizer JS, Wong KM, Manohar S, et al. Effects of acoustic trauma on the auditory system of the rat: the role of microglia. Neuroscience 2015; 303:299–311.

110. Day-Lollini PA, Stewart GR, Taylor MJ, et al. Hyperplastic changes within the leptomeninges of the rat and monkey in response to chronic intracerebroventricular infusion of nerve growth factor. Exp Neurol 1997;145:24–37.

111. Winkler J, Ramirez GA, Kuhn HG, et al. Reversible Schwann cell hyperplasia and sprouting of sensory and sympathetic neurites after intraventricular administration of nerve growth factor. Ann Neurol 1997;41:82–93.

112. Pizzo DP, Winkler J, Sidiqi I, et al. Modulation of sensory inputs and ectopic presence of Schwann cells depend upon the route and duration of nerve growth factor administration. Exp Neurol 2002;178:91–103.

113. Kaushal S, Tamer Z, Opoku F, et al. Anticonvulsant drug–induced cell death in the developing white matter of the rodent brain. Epilepsia 2016;57:727–734.

114. Bartha AI, Shen J, Katz KH, et al. Neonatal seizures: multicenter variability in current treatment practices. Pediatr Neurol 2007;37:85–90.

115. Bittigau P, Sifringer M, Genz K, et al. Antiepileptic drugs and apoptotic neurodegeneration in the developing brain. Proc Natl Acad Sci U S A 2002;99:15089–15094.

116. Katz I, Kim J, Gale K, et al. Effects of lamotrigine alone and in combination with MK-801, phenobarbital, or phenytoin on cell death in the neonatal rat brain. J Pharmacol Exp Ther 2007;322:494–500.

117. Kim J, Kondratyev A, Gale K. Antiepileptic drug-induced neuronal cell death in the immature brain: effects of carbamazepine, topiramate, and levetiracetam as monotherapy versus polytherapy. J Pharmacol Exp Ther 2007;323:165–173.

118. Forcelli PA, Kim J, Kondratyev A, et al. Pattern of antiepileptic drug-induced cell death in limbic regions of the neonatal rat brain. Epilepsia 2011; 52:e207–e211.

119. Brown L, Gutherz S, Kulick C, et al. Profile of retigabine-induced neuronal apoptosis in the developing rat brain. Epilepsia 2016;57:660–670.